NASA TN D-1191

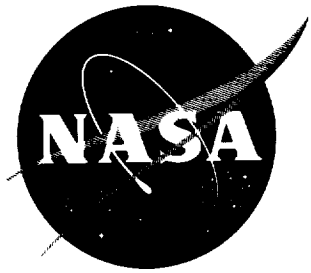

TECHNICAL NOTE
D-1191

MICROWAVE INTERFEROMETER MEASUREMENTS OF

ELECTRON-ION RECOMBINATION IN

NITROGEN, AIR, AND ARGON

By Perry Kuhns

Lewis Research Center
Cleveland, Ohio

NATIONAL AERONAUTICS AND SPACE ADMINISTRATION

WASHINGTON

February 1962

NATIONAL AERONAUTICS AND SPACE ADMINISTRATION

TECHNICAL NOTE D-1191

MICROWAVE INTERFEROMETER MEASUREMENTS OF ELECTRON-ION RECOMBINATION IN NITROGEN, AIR, AND ARGON

By Perry W. Kuhns

SUMMARY

Measurements of electron-density decay after an ionizing pulse were made, and electron-ion recombination coefficients were calculated from these values. Measurements were also made to show the effect of the introduction of water vapor on the recombination in air.

Data are given on the change in electron density with pressure of an abnormal glow discharge.

The theory of the propagation of an electromagnetic wave through a plasma is given along with the equations for using a microwave interferometer. Some of the practical considerations in using the microwave interferometer are presented.

INTRODUCTION

In the past few years there has been a considerable increase in interest in the effect of free electrons on the transmission characteristics of electromagnetic waves. This new interest has two reasons: first, the communication "blackout" of missiles due to the "plasma sheath" on reentry and to the ionization in the rocket exhaust during launch (refs. 1 to 3) and, second, the use of the transmission characteristics as a tool in the measurement of electron densities and temperatures of plasmas in fusion and electrical propulsion research (refs. 4 to 7).

The work reported in this paper was done primarily to study the mechanism of electron loss in plasmas, to study the problems of measuring electron densities by the microwave interferometer method, and to extend electron-ion recombination data to one decade lower in pressure. The results will be applicable mainly to measurements of plasmas obtained for electrical propulsion and communication loss studies.

The work reported in this paper consists of measurements of electron densities in a low-frequency, high-voltage discharge in the pressure range 0.04 to 0.8 millimeter of mercury and electron-ion recombination rate measurements on nitrogen, air, and argon in the range 0.3 to 7.0 millimeters of mercury. Some data are also given on the effect of water vapor on electron-ion recombination of air.

The first propagation studies of electromagnetic waves through an ionized gas were concerned with the reflection and cross-modulation of long radio waves by the ionosphere. Since then, full theoretical treatment of the propagation of electromagnetic waves through an ionized medium and the effect of ionization on electrical conductivity at high frequencies has been given in many texts (refs. 8 to 11) and published reports (refs. 12 to 16). A review of research on ionized media, including work with microwaves, may be found in reference 17. Surveys of plasma studies by means of microwaves may be found in references 18 and 19; these references contain bibliographies of work done up to approximately 1958 and 1960, respectively. Reference 20 is an earlier report of about the same scope.

There are four primary methods by which the transmission characteristics of an ionized medium may be studied.

The first method uses the free-space attenuation of an electromagnetic wave (refs. 21 to 24). This method is usually used in a medium at pressures above 20 millimeters of mercury. The gas is seeded with some easily ionized material such as an alkali salt, and there is a high enough collision rate between electrons and other particles to dissipate the microwave energy.

The second method uses the change in resonant frequency and band width of a tuned cavity or waveguide structure (refs. 25 to 30). This method is usually used on small confined discharges and ones with fairly high collision rates.

The third method uses cross-modulation, in which a small signal will experience an attenuation because of a large signal's changing the electron-collision frequency of the ionized medium (refs. 31 and 32). Again, fairly high collision rates are found.

The fourth method, the method used in this report (fig. 1), uses the change in the wavelength of the microwaves in the medium due to the presence of free electrons. This method usually uses a microwave interferometer for the measurement (refs. 5, 6, and 33 to 38); the electron-collision frequency is kept low so that there is no attenuation.

With this method a larger confining space can be used, and electron-density and electron-ion-recombination-coefficient measurements may be extended to lower pressures than when the cavity method is used.

THEORY

Electromagnetic Wave Propagation

The theory for the propagation of a plane electromagnetic wave in a homogeneous, weakly ionized medium has been treated in many texts and reports (refs. 8 to 14, and 23). No attempt will be made here to develop the theory fully.

The differential equation for a plane wave propagating in the z-direction in an unbounded plasma is

$$\frac{\partial^2 E}{\partial z^2} - \mu\epsilon \frac{\partial^2 E}{\partial t^2} - \mu\sigma \frac{\partial E}{\partial t} = 0 \tag{1}$$

(All the symbols are defined in the appendix.) In developing equations, the rationalized MKS system is used. However, final equations may also be shown in other more practical units. When this is done, the units to be used are denoted by subscript on the appropriate symbol.

If the wave is harmonic, then the solution to equation (1) is given by

$$E = E_o \exp(j\omega t - j\beta z - \alpha z) \tag{2}$$

$$(\alpha + j\beta)^2 = -\mu\epsilon\omega^2 + j\mu\sigma\omega \tag{3}$$

In equation (2), $\exp(-j\beta z)$ is the equation of a wave in space and can be written as $\exp(2\pi z/\lambda)$; thus, the wavelength λ is given by $\lambda = 2\pi/\beta$, where β is a phase constant. The part $\exp(-\alpha z)$ is an attenuation in space; α is then an attenuation coefficient.

The equation for the motion of an electron in an electric field that is polarized in the y direction is

$$\frac{m d^2 y}{dt^2} + m\omega_c \frac{dy}{dt} = e E'_o \exp(j\omega t) \tag{4}$$

In this equation, ω_c is a damping term that is equal to the collision frequency between electrons and atoms or ions and will be assumed to be a constant. The solution is given by

$$y = \frac{1}{\omega_c + j\omega} \frac{je}{\omega m} E'_o \exp(j\omega t) \tag{5}$$

The current density is given by

$$J = ne\frac{dy}{dt} = \frac{ne^2}{\omega_c + j\omega}\frac{E}{m} \tag{6}$$

or, since $J = \sigma E$,

$$\sigma = \frac{n\frac{e^2}{m}}{\omega_c + j\omega} \tag{7}$$

If it is assumed that both ϵ and μ are unaffected by the free electrons, then substitution of (7) into (3) gives the following solutions for α and β:

$$\alpha = \frac{\omega}{c}\left\{\frac{1}{2}(1 - \varphi)\left[-1 + \sqrt{1 + \left(\frac{\varphi\omega_c}{\omega(1 - \varphi)}\right)^2}\right]\right\}^{1/2} \tag{8}$$

$$\beta = \frac{\omega}{c}\left\{\frac{1}{2}(1 - \varphi)\left[1 + \sqrt{1 + \left(\frac{\varphi\omega_c}{\omega(1 - \varphi)}\right)^2}\right]\right\}^{1/2} \tag{9}$$

where

$$\varphi = \frac{\omega_p^2}{\omega_c^2 + \omega^2} \qquad \text{and} \qquad \varphi \leq 1 \tag{10}$$

The quantity ω_p is the "plasma frequency" and is given by

$$\omega_p^2 = \frac{ne^2}{m\epsilon} \cong 3.18\times10^9 n_{cc} \tag{11}$$

In most work the number of collisions is small compared with the frequency of radiation ($\omega_c \ll \omega$). When this is true, and if $\varphi < 1$, equations (8), (9), and (10) may be simplified to

$$\alpha \simeq \frac{1}{2}\frac{\omega_c}{c}\frac{\varphi}{\sqrt{1 - \varphi}} = \frac{\pi}{\lambda_{vac}}\frac{\varphi}{\sqrt{1 - \varphi}}\frac{\omega_c}{\omega} \tag{8a}$$

$$\beta \simeq \frac{\omega}{c}\sqrt{1 - \varphi} = \frac{2\pi}{\lambda_{vac}}\sqrt{1 - \varphi} = \frac{2\pi}{\lambda_p} \tag{9a}$$

$$\varphi \simeq \left(\frac{\omega_p}{\omega}\right)^2 \tag{10a}$$

The effect of the plasma density on attenuation and plasma wavelength is shown in figure 2.

Two things can now be seen. First, when $\omega_p \ll \omega$, there will be little or no attenuation until $\omega_p \cong \omega$; then α becomes large for microwave frequencies (cutoff). Second, as the number of electrons gets larger, β gets smaller or, to put it another way, the index of refraction becomes less than unity since

$$\eta = \frac{\lambda_{vac}}{\lambda_p} = \frac{\beta_p}{\beta_{vac}} = \sqrt{1 - \varphi} \tag{11}$$

When $\varphi > 1$ (above cutoff), the equation for α is equation (9) with $(1 - \varphi)$ replaced by $(\varphi - 1)$, and the equation for β is equation (8) with $(1 - \varphi)$ replaced by $(\varphi - 1)$.

Interferometer Equations

To measure the change in the index of refraction, an interferometer is used. The interferometer is set up as shown in the schematic diagram of figure 1; P_1, P_2, and P are the power in each arm (P_2 the plasma arm) and the power due to transmission through both arms. The output of the detector, a crystal diode, is proportional to the power. Thus, three variables are measured: P_1, P_2, and P. Without any plasma $P_{1,o}$ and $P_{2,o}$ are set, and the phase angle between them is varied to obtain the desired θ_o and P_o:

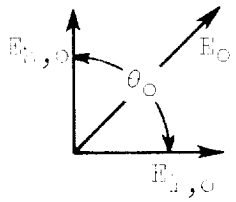

$$\frac{P_o}{P_{1,o}} = \frac{E_o^2}{E_{\perp,o}^2} = \left(1 + 2\sqrt{\frac{P_{2,o}}{P_{\perp,o}}}\cos\theta_o + \frac{P_{2,o}}{P_{\perp,o}}\right) \tag{13}$$

$$\cos\theta_o = \frac{\dfrac{P_o}{P_{1,o}} - \left(1 + \dfrac{P_{2,o}}{P_{\perp,o}}\right)}{2\sqrt{\dfrac{P_{2,o}}{P_{1,o}}}} \tag{14}$$

When there is a plasma, the wavelength of the microwaves becomes longer in the plasma:

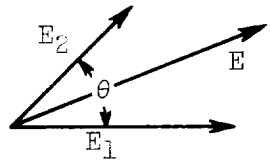

$$\frac{P}{P_1} = 1 + 2\sqrt{\frac{P_2}{P_1}}\cos\theta + \frac{P_2}{P_1} \tag{14a}$$

In equations (13) and (14), P_o is now P, and so forth. The quantity that is usually determined is the phase shift $\Delta\theta$. The equation for θ can be written in terms of θ_o and $\Delta\theta$:

$$\cos\theta = \cos(\theta_o + \Delta\theta) = \cos\left[\theta_o + l\left(\frac{2\pi}{\lambda_p} - \frac{2\pi}{\lambda_{vac}}\right)\right] \tag{15}$$

or, since

$$\frac{2\pi}{\lambda_p} \cong (-\sqrt{1-\varphi})\left(\frac{2\pi}{\lambda_{vac}}\right)$$

$$-\sqrt{1-\varphi} \cong 1 + \frac{\lambda_{vac}}{2\pi}\frac{\Delta\theta}{l} \tag{16}$$

or, when $\omega_c \ll \omega$ and $\varphi \ll 1$,

$$n_{cc} \cong 2.07\times10^9 f_{Gc}\left(\frac{\Delta\theta_{deg}}{l_{cm}}\right) \tag{17}$$

If there is attenuation due to collisions and if $\omega_c/\omega < 1$, then

$$\frac{\omega_c}{\omega} \cong \frac{28.7}{\Delta\theta_{deg}}\frac{\Delta P}{P_{2,o}} \tag{18}$$

$$n_{cc} \cong 2.07\times10^9 f_{Gc}\left(\frac{\Delta\theta_{deg}}{l_{cm}}\right)\left[1 + \left(\frac{\omega_c}{\omega}\right)^2\right] \tag{19}$$

The power P as a function of the phase difference $\Delta\theta$ is shown in figure 3 for different values of P_2/P_1.

Mechanism of Loss of Free Electrons

There is an extensive amount of literature dealing with the mechanism of electron loss in gases and its application to discharges. For this reason, no detailed analysis is given here. Instead, the reader is referred to references 39 to 43.

The rate of electron loss in an electrically neutral ionized gas is given by

$$\frac{\partial n}{\partial t} = D_a \nabla^2 n - C_R n^2 - g\omega_c n \tag{20}$$

where

$D_a \nabla^2 n$ loss due to ambipolar diffusion to, and recombination at, the walls of the container

$C_R n^2$ loss due to electron-ion recombination either by three-body and dissociative or radiative collision

$g\omega_c n$ loss due to electron - neutral particle attachment at higher pressures, due mostly to the presence of impurities

Three simple solutions to this equation are of interest here:

(1) The solution when diffusion loss is predominant. The solution is a function of the geometry of the container for the lowest diffusion mode in a circular cylinder:

$$n = n_o \sin \frac{\pi h}{H} J_0\left(\frac{2.405r}{R}\right) \exp(-t/\tau) \tag{21}$$

where

$$\frac{1}{D_a \tau} = \left(\frac{\pi}{H}\right)^2 + \left(\frac{2.405}{R}\right)^2 \tag{22}$$

By plotting the logarithm of n against t, the value of τ and (from eq. (25)) the diffusion coefficient D_a may be found. Since the diffusion coefficient is proportional to the mean free path and the mean velocity, the coefficient $D_a \propto \frac{1}{p} T^{3/2}$ (refs. 39 and 41) at low pressures.

(2) The solution when electron-ion recombination is predominant. This solution is independent of geometry:

$$\frac{1}{n} - \frac{1}{n_o} = C_R(t - t_o) \tag{23}$$

By plotting $1/n$ against t, the value of C_R may be obtained. If the recombination coefficient C_R is proportional to the collision cross section for electron-ion collisions, C_R is proportional to $(p)^{1/2}$ for N_2 and proportional to p for rare gases (ref. 41). If the recombination is of the three-body type, then C_R is proportional to p at low pressures (refs. 39 and 41).

(3) The solution when both electron-ion recombination and attachment to impurities are equally important. In this case, $\omega_c = KN_m$ and the solution becomes:

$$\frac{1}{n} - \frac{1}{n_o} = C_R(t - t_o)\left(1 + 2\frac{gK}{C_R} - \frac{gK}{C_R}\frac{N_{m,o}}{n_o}\right) \tag{24}$$

when a small amount of impurity is present. If the attachment to the impurity is strong (g large), then the additional terms cannot be neglected. When this happens, it is necessary to obtain plots of $1/n$ against t at different values of the initial electron density in order to separate the two processes of electron loss.

Other solutions in which any two of the preceding processes are present are given in reference 41. The effects on the transmission characteristics of electromagnetic waves of an ionized gas as the gas goes from a homogeneous gas (independent of r) to a diffusion-loss-dominated gas $r = f(r)$ after a discharge is given in reference 28.

PRACTICAL CONSIDERATIONS

Frequency To Be Used

The maximum electron density that can be measured is theoretically given by the cutoff frequency,

$$(n_{cc})_{max} \cong 1.2\times10^{10} f_{Gc}^2 \tag{25}$$

The lower limit is given by the ability to detect a small phase-angle change. By setting the phase angle so that one is on the steep part of the curve in figure 4 and by making $P_2/P_1 > 1$, a minimum angle of about 5° can be accurately detected, or

$$(n_{cc})_{min} \cong \frac{10^{10} f_{Gc}}{l_{cm}} \tag{26}$$

These limits can, of course, be changed by the presence of magnetic fields or by collisions.

Collision Frequencies

Absorption of the microwave beam by the plasma only becomes appreciable near cutoff or when $\omega_c/\omega \cong 1$; this can be seen in figure 2. Also, it is seen that, when $\omega_c/\omega \cong 1$, the index of refraction of the plasma stays close to 1. The medium is then absorptive. The energy the electrons obtain from the electromagnetic wave is dissipated in collisions with atoms or ions. When this is true, the method of measurement is usually by the attenuation of a microwave beam, or corrections must be made to formulas to allow for collisions (eqs. (18) and (19)).

To estimate collisions between electrons and atoms (molecules), the classical hard-sphere formula may be used (refs. 44 and 45) in the low-temperature range ($T_e \gtrsim 0.1$ ev).

$$\omega_c \cong \bar{v}\, Q_e \cong 5.3\times10^{7} d_{cm}^{2} N_{cc} \sqrt{T_e} \tag{27}$$

$$d_{cm} \cong 3\times10^{-8} \text{ cm}$$

The quantity T_e is in ev, and N_{cc} is in cc^{-1}. Since in the present work $\omega \cong 5\times10^{10}$ to make $\omega_c/\omega \cong 1/2$, N must equal 10^{18} or approximately 0.1 atmosphere pressure. Using electron-collision cross sections at low energy (ref. 38) or the more complex method of Margenau (ref. 12), approximately the same answer is obtained for weakly ionized gases. Thus, electron-atom collisions may be neglected at room temperature. For higher energy ($T_e > 0.1$ ev) the published data on electron-collision cross sections should be used, and care should be taken to differentiate between the cross sections for energy transfer and for momentum transfer (refs. 38 and 41).

To calculate electron-ion collision rates, either of the two formulas (28a) or (29b) is applicable for a weakly ionized gas where the ions are singly ionized:

$$\omega_c \cong 1.05\times10^{-5} \frac{N_i}{T_i^{3/2}} \log_{10} \frac{2.53\times10^{6} T_e}{n^{1/3}} \tag{28a}$$

(refs. 45 and 46)

$$\omega_c \cong 6.8\times10^{-6} \frac{N_i}{T_i^{3/2}} \log \frac{1.40\times10^{10} T_e}{n^{1/2}} \tag{28b}$$

(ref. 47).

Two other formulas for the collision frequency may be found in references 48 and 49. The magnitude of the theoretical value of ω_c depends greatly on the assumption as to what constitutes a collision. The two formulas just given check well with data given in reference 47. Values given by the formulas in reference 49 are about three times higher and that of reference 48 is 10 times lower than that of equation (28a) or (28b).

Again, for ions to make $\omega_c/\omega \cong 1/2$,

$$N_i \cong 1.2 \times 10^{14} \quad \text{at} \quad T = 0.2 \text{ ev}$$

which is beyond the cutoff frequency density of the present interferometer if $n \cong N_i$.

When $\omega_c/\omega \ll 1$, the interferometer method is used and the equations presented for it are used. In this type of medium the wavelength is larger than that in free space; and refraction, reflection, and scattering take place but no absorption.

Existence of Thermal Equilibrium

While the collision frequency between electrons and molecules is given by ω_c, the fraction of energy exchanged with each collision is of the order of m/M. Thus, the time for a Maxwellian electron gas at one temperature to reach the temperature of a Maxwellian distribution of molecules is given by the differential equation

$$\frac{d(T_e - T_\infty)}{dt} \cong -\omega_{c,\infty}\left(\frac{T_e}{T_\infty}\right)^{1/2}(T_e - T_\infty)\frac{m}{M} \tag{29}$$

where the additional effect of the electron temperature on the collision frequency is included. This equation may be solved in parts to obtain the curves of $(T_e - T_\infty)$ against tp given for nitrogen in figure 4. Since the dependence of C_R on temperature has been found to be proportional to $T^{0.9}$ (ref. 50), a correction can be made to data obtained at short times. As can be seen from figure 4, the temperature difference becomes small and can be neglected for values of $tp > 60$ (μsec)(mm Hg).

All the preceding presupposes that both the electron and molecule energy distributions are Maxwellian. This may not necessarily be true; indeed, in low electron-density gases the collision rate between electrons is of the order of the collision rate between electrons and ions. In such cases, the electrons that first recombine will be those of low energy, with the higher energy electrons possibly exciting molecules upon collision sufficiently to cause additional ionization. A more detailed discussion of this problem may be found in references 49 and 51.

The considerations so far discussed are of a general nature and depend on the type of discharge to be studied. There are other considerations that depend more on the construction and dimensions of the physical apparatus.

Inhomogeneity of the Plasma

The theory so far developed is for a plane wave in a homogeneous plane plasma. If the waves and plasma are plane but the plasma varies along the path length, then the phase change is an integral along the path:

$$\Delta\theta \cong \int \left(\frac{2\pi}{\lambda} - \frac{2\pi}{\lambda_p}\right) dl = \frac{2\pi}{\lambda_{vac}} - \alpha \; dl \qquad (30)$$

For small values of $\Delta\theta/l$ the electron density is an average over the length. This integral has been evaluated in reference 33. For a cylindrical confining chamber, N_{av} is equal to 0.61 times the center value of n for the lowest diffusion mode.

If the wavelength and dimensions are such that a diverging beam through an inhomogeneous cylinder must be considered, the problem is quite complex. If there are sufficient collisions so that $\omega_c/\omega \gtrsim 1$, the medium is not refractive but absorptive; and, again, straight integration can be used if it is assumed that the beam shape is not changed passing through the medium. Some evaluations of this type of inhomogeneity may be found in reference 23.

Beam Size and Path Length

The size of the beam depends on the radiator used. If lenses are used that focus through windows, the minimum beam width is approximately λ. If only horns are used, the beam sampling width will be approximately the horn dimensions. When a cylindrical container is used, care must be taken that the main power lobe from the horn or lens does not strike the container side walls.

To avoid standing waves, the path length should be at least 5 wavelengths and the separation between horns and lenses at least five times their dimensions. The values given are the minimal values, and errors will still be introduced. Error can be reduced by making measurements at a number of power settings, phase angles, frequencies, and at different tuning.

Power Loss Due To Reflections and Standing Waves

The equations developed have been for a wave in an unbounded medium. This, of course, is never true. Boundaries to the plasma will produce reflections from the plasma and standing waves in it. The formulas for effects of reflections from the boundaries and standing waves are given in references 8 and 14, from which the magnitude of such effects may be calculated.

It is usually necessary to confine the plasma region physically in a container and provide windows for the passage of the microwaves into the plasma. If the plasma is such that there is a discontinuity at the window, the reflections from the window will change with plasma density. This effect can be minimized by using half-wave windows or, when this cannot be done, by placing a ferrite isolator in the sending arm of the interferometer or by keeping the plasma away from the windows by magnetic fields, and so forth.

If the container is large compared with the radiation wavelength and the plasma density is limited by diffusion to the walls, the discontinuity will not be present.

If the horns, lenses, or windows are so close that standing waves are set up between them, another effect takes place. As the density of the plasma changes, the number of standing waves in the plasma changes. As a result the received power has a sinusoidal variation; this variation may even be used as a crude measure of electron density. This effect may be lessened by careful tuning and the use of high transmission windows. However, usually the result will be to lower the maximum measurable density below the cutoff density (eq. (25)).

EXPERIMENTAL METHODS

Apparatus

A schematic diagram of the microwave interferometer apparatus is shown in figure 1.

The frequencies used in the measurements were X-band (9 Gc) and K-band (22 Gc). The average electron densities measured varied from 2×10^{10} to 10^{11} cc^{-1} with 9 Gc, and from 10^{10} to 3×10^{11} cc^{-1} with 22 Gc. The lower limit of electron density was determined by the sensitivity of the system to measure small phase-angle changes. The upper limit was set by standing waves in the container, especially for X-band measurements.

The power ratios of the phase angle between the two arms were set in the region so marked in figure 3.

The ionized gas was confined inside a 15-centimeter-diameter Pyrex tube approximately 100 centimeters long. The gas pressure varied from 0.04 to 7.0 millimeters of mercury. The microwave measurements were made either through the walls of the Pyrex tube or through Lucite windows in a Pyrex cross. The distance between horns (no lenses were used) varied from 15 to 20 centimeters. In no case was the power of the measuring radiation strong enough to affect the discharge. Three gases were used: nitrogen, air, and argon.

Techniques

Two techniques were used to ionize the gas:

(1) Ionization by a-c abnormal glow discharge: Data were obtained using a 60-cycle-per-second discharge between two cooled copper electrodes of approximately 7-centimeter diameter separated by approximately 20 centimeters. For this experiment the voltage between electrodes was maintained at a 6300-volt peak. The root mean square current of the discharge is shown as a function of the pressure in figure . This discharge was diffusion or recombination controlled, depending on the pressure. The electron temperature was high (approx. 2 ev) (refs. 39 and 41).

For the measurement of electron density the microwave power was square-wave modulated at approximately 1800 cycles per second, and the peak value was read from an oscilloscope screen. Because of the high electron temperature, a small correction varying from 1 to 10 percent was made to the X-band data because the collision rate approached the radiation frequency (eqs. ( ) and (27)). Equation (17) was used for K-band data.

A check on the measured electron density of nitrogen was made in the following manner. By integrating $J_0(2.405\ r/R)$ of equation (21), a relation between the peak current and the measured electron density n was obtained; $i_{peak} \approx 2.2\ ev_d n$. The peak current is obtained from the root mean square measured current from oscilloscope traces of electron density with time. The current is proportional to voltage times electron density. The trace curve is multiplied by the instantaneous voltage, squared, and integrated to obtain a ratio of i_{RMS} to i_{peak}. Using the value of v_d found in reference 39 for nitrogen at a given voltage and the calculated i_{peak}, the electron density was calculated.

All measurements of electron density were made in the positive column of the discharge.

(2) Ionization by pulsed radar: Data on electron-ion recombination coefficients were obtained by measuring the decay of electron density after an S-band (3Gc) pulse of 1-megawatt peak power, 620 pulses per

second, and 1-microsecond pulse width had ionized the gas. Data were taken in the pressure range 0.3 to 7.0 millimeters of mercury. The electron temperature for this type of discharge is low (approx. 0.03 ev) (refs. 37 and 38).

For these measurements unmodulated microwave power was used, the crystal output was displayed on an oscilloscope with a total time for a trace varying from 25 to 500 microseconds, and the data were reduced from photographs of the screen. Most of the data were taken with K-band because of the high electron densities, and no correction was made for electron collisions.

It was found with nitrogen that, when data taken with X- and K-band disagreed at high pressures or at high power input, the discharge no longer looked homogeneous when sighted along the cylindrical axis. This lack of visual homogeneity was used then with nitrogen and the other gas to determine when data should not be taken because of high power or pressure. A homogeneous discharge could not be obtained for nitrogen or air at pressures above 1.3 millimeters of mercury, and above 7.0 millimeters of mercury for argon.

RESULTS

Steady-State Data

Shown in figure 6 are the measured average electron densities at peak voltage for X- and K-band measurements of the three gases as a function of the gas pressure. As was expected, below approximately 0.2 millimeter the discharge is diffusion-controlled ($n \propto p$), while above that pressure the discharge is recombination-controlled ($n \propto 1/p$). A check on the measured densities of electrons in nitrogen was made at two pressures using the method outlined before. The two calculated points are shown in figure 6(a). In the region where the discharge is truly a glow discharge (0.085 mm), the measured and calculated values agree closely. In the region of abnormal glow there is a large discrepancy, which is probably due to the fact that in the abnormal glow the cathode fall is much larger; thus, the voltage drop across the positive column is smaller. This in turn would lower the drift velocity v_d and thus increase the electron density.

The disagreement between X- and K-band data at higher electron densities is due to the effect of increased scattering and detuning.

Time-Dependent Data

Data were taken on three gases, nitrogen, air, and argon, to obtain the electron-ion recombination coefficient (C_R, eq. (24)).

Nitrogen. - Measurements were made in the pressure range 0.15 to 1.6 millimeters of mercury. The values of C_R obtained from these measurements are shown in figure 7(a) as a function of the pressure in the chamber. Also shown are values of C_R for higher pressures obtained by Biondi and Brown (ref. 50) using the cavity method of electron-density measurement.

The gas used for these measurements was obtained from bottles that are filled by passing liquid nitrogen through a heat exchanger, and is reported to be 99.99 percent pure. From the bottle the gas is passed through an acetone - dry-ice trap and through a vacuum valve into the chamber. A small amount of hydrocarbon in the gas due to improper outgassing of the chamber was found to increase C_R by a factor of about 2 to a constant value of 1.5 to 1.7×10^{-6} in the pressure region measured. A small amount of air leakage was found to lower the value of C_R at high pressures and to make C_R directly proportional to the pressure in the middle and lower pressure regions.

While it is felt that the data do exhibit the expected dependence on p, some of this may still be due to the introduction of impurities due to back-diffusion after the chamber has been purged.

No temperature correction was made to the values of C_R shown, as either the times were sufficient to assure thermal equilibrium or the plot of $1/n$ against time did not exhibit any characteristic change due to temperature. Short-term data (sweep rate, 5 μsec/cm) and long-term data (sweep rate, 20 μsec/cm) agreed to the extent that it is felt that electrons undergoing recombination were only those at the lower end of the energy distribution.

Air. - Measurements were made in the pressure range 0.2 to 1.0 millimeter of mercury. The values of C_R obtained are shown in figure 7(b) plotted as a function of the partial pressure of oxygen.

The gas used in these experiments was either room air or bottled air passed through an acetone - dry-ice trap. No difference was found in C_R because of the difference in gas source. It is seen that the recombination coefficient is about 10 times smaller than that found for nitrogen. Also plotted in figure 7(b) are values of C_R for oxygen from reference 50. The agreement of these data with that of this report for air suggests that the ionization and recombination observed was that of oxygen.

Argon. - Measurements were made in the pressure range 0.6 to 7.5 millimeters of mercury. The values of C_R obtained are shown in figure 7(c).

The gas used in these experiments was commercial-grade argon at approximately 99.9-percent purity. Some water vapor was present in the bottled gas, as data taken without the trap were some five times higher than the data shown. Good agreement was obtained with low-pressure data of reference 52, and a trend toward the higher pressure data was shown. The data are not extensive enough to show what the pressure dependence of C_R is; however, $C_R \propto p$ looks probable.

Effect of Water Vapor on Electron-Ion Recombination

The decay of electron density with time for air with various amounts of water vapor present as an impurity is shown in figure 8. The water was introduced into the air by bubbling the dried air through water at various pressures. The percentage of water given in figure 8 assumes that the air was saturated. As can be seen from the figure, the effect is very strong, which is expected (ref. 43), raising the effective C_R by a factor of 10 with the introduction of about 3 percent H_2O by volume. The ionization potentials of O_2 and H_2O are comparable (ref. 53), at 12.5 electron volts, so that the O_2 is still probably the dominant gas being ionized; when only a small percentage of water is in the air, however, the collision cross section of H_2O is some 10 times larger than that of any other constituent of air (ref. 41), so that collisions with the introduction of H_2O are more frequent and, in fact, are dominant. Also, such collisions may be more effective because of the shape of the H_2O molecule. Another process probably enters into the decay also - that of electron attachment to the H_2O molecule.

SUMMARY OF RESULTS

Electron-density measurements were made of a high-voltage discharge by means of microwave interferometers at two wavelengths. Good agreement was shown over the entire range between experimental results at the two wavelengths; agreement was also obtained with the theory of such discharges at the low-pressure (glow discharge) region. Plots of electron density against pressure show the transition from diffusion-loss-controlled discharge to a recombination-controlled discharge.

Measurements were made of electron-density decay after an ionizing pulse, from which the electron-ion recombination coefficient C_R was calculated. Agreement with previous data using the cavity technique was good, and the value of C_R was extended downward by a factor of 5. Comparison of air-recombination values with those for oxygen suggest that

the ionization which predominated was that of oxygen. Agreement of argon data was good in the low-pressure range, and a pressure trend was shown that approaches the data at higher pressures taken by means of the cavity method.

Measurements were also made to show the effect of the introduction of water vapor on the electron-ion recombination of air. A strong effect was found; reasons are presented for the magnitude of this effect.

Lewis Research Center
National Aeronautics and Space Administration
Cleveland, Ohio, November 6, 1961

APPENDIX - SYMBOLS

c	velocity of light in a vacuum, 2.998×10^8 m/sec
C_R	recombination coefficient
D_a	ambipolar diffusion coefficient
d	collision diameter
E	electric field intensity
E_o'	$E_o \exp(-j\beta z - \alpha z)$
e	electronic charge, 1.602×10^{-19} coulomb
f_{Gc}	radiation frequency, 10^9 cps
g	efficiency of attachment to an impurity
H	tube length
h	distance along tube length
i	current
J	current density
J_o	zero-order Bessel function
K	impurity constant
l	path length
M	heavy-particle (atom or molecule) mass
m	electron mass, 9.107×10^{-31} kg
N	heavy-particle density
n	electron density
P	power
p	pressure
Q_e	electron-collision cross section

R	tube radius
r	radial distance
T	temperature, ev (1 ev $\cong$ 11,400^{o} K)
t	time
$\overline{v}$	mean velocity
v_d	drift velocity
x,y,z	coordinates
α	attenuation constant
β	phase constant
ϵ	permittivity of free space, 8.85×10^{-12} farad/meter
η	index of refraction
θ	phase angle
λ	wavelength
μ	permeability of free space, 1.257×10^{6} henrys/meter
σ	conductivity
τ	time constant
φ	$\frac{\omega_p^2}{\omega_c^2 + \omega^2}$
ω	radiation frequency, (radians)(sec^{-1})
ω_c	collision frequency
ω_p	plasma frequency

Subscripts:

e	electron
i	ion
m	impurity

o	initial
p	plasma
vac	vacuum
1	unaffected arm of interferometer
2	plasma arm of interferometer
∞	final

NOTE: Subscripts are also used to denote dimensions in numerical formulas.

REFERENCES

1. Anon.: The Plasma Sheath - Its Effect on Communications and Detection. Proc. of Symposium on the Plasma Sheath, vol. I, Dec. 7-9, 1959.

2. Sanger, E., Goercke, P., and Bredt, I.: On Ionization and Luminescence in Flames. NACA TM 1305, 1951.

3. Balwanz, W. W.: Interaction Between Electromagnetic Waves and Flames. Pt. 6 - Theoretical Plots of Absorption, Phase Shift, and Reflection. Rep. 5388, Naval Res. Lab., Sept. 23, 1959.

4. Brown, S. C.: Microwave Studies of Gas Discharge Plasmas. Vol. 32 of Int. Conf. on Peaceful Uses of Atomic Energy, 1958, pp. 394-397.

5. Drummond, James E.: Theory of Microwave Diagnostics of Hot Plasmas. Vol. 32 of Int. Conf. on Peaceful Uses of Atomic Energy, 1958, pp. 379-384.

6. Wharton, Charles B.: Microwave Diagnostics for High-Temperature Plasmas. Rep. 4836, Radiation Lab., Univ. Calif., Mar. 1957. (See also ch. 12 of Plasma Phys., James E. Drummond, ed., McGraw-Hill Book Co., Inc., 1961.)

7. Anoshkin, V. A., et al.: Microwave Investigations of Plasma on the "Alpha" Device. Soviet Phys.-Tech. Phys., vol. 5, no. 12, June 1961, pp. 1370-1377.

8. Stratton, J. A.: Electromagnetic Waves. McGraw-Hill Book Co., Inc., 1941.

9. Bremmer, H.: Propagation of Electromagnetic Waves. Handbuch der Phys., S. Flugge, ed., vol. XVI, Springer-Verlag, 1958, pp. 423-638.

10. Montgomery, C. G., Dicke, R. H., and Purcell, E. M., eds.: Principles of Microwave Circuits. McGraw-Hill Book Co., Inc., 1948.

11. White, F. W. G.: Electromagnetic Waves. Meuthen and Co., 1950.

12. Margenau, H.: Conduction and Dispersion of Ionized Gases at High Frequencies. Phys. Rev., vol. 69, nos. 9-10, May 1-15, 1946, pp. 508-513.

13. Whitmer, R. F.: Principles of Microwave Interactions with Ionized Media. 1 - Plasma Resonance. The Microwave Jour., vol. 2, no. 2, Feb. 1959, pp. 17-19. (See also pt. II, vol. 2, no. 3, Mar. 1959, pp. 47-51.)

14. Jahn, Robert G.: Interaction of Electromagnetic Waves with Ionized Gases. TN 59-911, Office Sci, Res., Aug. 1959.

15. Margenau, Henry: Conductivity of Plasmas to Microwaves. Phys. Rev., vol. 109, no. 1, Jan. 1, 1958, pp. 6-9.

16. Desloge, Edward A., Matthysse, Steven W., and Margenau, Henry: Conductivity of Plasmas to Microwaves. Phys. Rev., vol. 112, no. 5, Dec. 1, 1958, pp. 1437-1440.

17. Rix, H. D.: Radio Propagation and Ionized Gases - A Survey. Sci. Rep. 123, pt. A, Penn. State Univ., Sept. 1, 1959.

18. Raizer, M. D., and Shpigel, I. S.: Study of Plasma by Means of Micro Radio Waves. Uspekhi Fizicheskikh Nauk, vol. 64, no. 4, Apr. 1958, pp. 641-667. (English Trans. AEC TR-3584.)

19. Golant, V. E.: Microwave Plasma Diagnostic Techniques. Soviet Phys.-Tech. Phys., vol. 5, no. 11, May 1961, pp. 1197-1248.

20. Goldstein, L.: Electrical Discharge in Gases and Modern Electronics. Advances in Electronics and Electron Phys., vol. VII, Academic Press, 1956.

21. Belcher, H., and Sugden, T. M.: Studies on the Ionization Produced by Metallic Salts in Flames. 1 - The Determination of the Collision Frequency of Electrons in Coal-Gas/Air Flames. Proc. Roy. Soc. (London), ser. A., vol. 201, no. 1067, May 1950, pp. 480-488. (See also pt. II, ser. A, vol. 202, no. 1068, June 1950, pp. 17-39.)

22. Rudlin, Leonard: Preliminary Results of a Determination of Temperatures of Flames by Means of K-Band Microwave Attenuation. NACA RM E51G20, 1951.

23. Kuhns, Perry W.: Determination of Flame Temperatures from 2000° to 3000° K by Microwave Absorption. NACA TN 3254, 1954.

24. Huber, Paul W., and Gooderum, Paul B.: Experiments with Plasmas Produced by Potassium-Seeded Cyanogen Oxygen Flames for Study of Radio Transmission at Simulated Reentry Vehicle Plasma Conditions. NASA TN D-627, 1960.

25. Biondi, Manfred A., and Brown, Sanborn C.: Measurements of Ambipolar Diffusion in Helium. Phys. Rev., vol. 75, no. 11, June 1, 1949, pp. 1700-1705.

26. Brown, Sanborn C., and Rose, David J.: Methods of Measuring the Properties of Ionized Gases at High Frequencies, pts. I, II, and III. Jour. Appl. Phys., vol. 23, no. 7, July 1952, pp. 711-718; 719-722; vol. 23, no. 9, Sept. 1952, pp. 1028-1032.

27. Udelson, Burton S., Creedon John E., and French, Judson C.: Microwave Measurements of the Properties of a dc Hydrogen Discharge. Jour. Appl. Phys., vol. 28, no. 6, June 1957, pp. 717-723.

28. Oskam, H. S.: Microwave Investigation of Disintegrating Gaseous Discharge Plasmas. Philips Res. Reps., vol. 13, 1958, pp. 335-457.

29. Buchsbaum, S. J., Mower, Lyman, and Brown, Sanborn C.: Interaction Between Cold Plasmas and Guided Electromagnetic Waves. The Phys. of Fluids, vol. 3, no. 5, Sept.-Oct., pp. 806-819.

30. Brown, S. C.: Plasma Research at M.I.T. Plasma Phys., J. E. Drummond, ed., McGraw-Hill Book Co., Inc., 1961.

31. Goldstein, L., Anderson, J. M., and Clark, G. L.: Interaction of Microwaves Propagated Through a Gaseous Discharge Plasma. Phys. Rev., vol. 90, no. 1, Apr. 1, 1953, pp. 151-152. (See also vol. 90, no. 3, May 1, 1953, pp. 486-487.)

32. Anderson, J. M., and Goldstein L.: Variation with Electron Energy of the Collision Cross Section of Helium for Slow Electrons. Phys. Rev., vol. 102, no. 4, May 15, 1956, pp. 933-938.

33. Wharton, Charles B.: Microwave Interferometer Measurements for the Determination of Plasma Density Profiles in Controlled Fusion Experiments. UCRL-5400, Radiation Lab., Univ. Calif., Nov. 6, 1958.

34. Heald, Mark A.: The Application of Microwave Techniques to Stellarator Research. MATT-17, Princeton Univ., Aug. 26, 1959.

35. Heald, Mark A.: Engineering Design of Microwave Electron Density Measuring Systems. Tech. Memo. 78, Princeton Univ., July 6, 1959.

36. Kannelaud, Jean, and Whitmer, Romayne F.: Improved Microwave Techniques for Measuring Plasma Parameters. Sci. Rep. 1, Sylvania Electric Products, Inc., July 22, 1959.

37. Ernst, W. P.: An Electron Density Measuring System for Hot Plasma Research. The Microwave Jour., vol. 4, no. 2, Feb. 1961, p. 49.

38. Holt, E. Howard: Semiannual Status Report No. 2. NASA Grant NsG48-60, May 1-Oct. 31, 1960, Rensselaer Polytech. Inst., Mar. 1961.

39. Von Engel, A.: Ionized Gases. Claredon Press (Oxford), 1955.

40. Anderson, J. M.: Electron-Ion Recombination in Low-Temperature Gaseous Plasma - A Survey of Experimental Work. Rep. 61-RL-2817G, General Electric Co., Sept. 1961.

41. Brown, Sanborn Conner: Basic Data of Plasma Physics. Technology Press, M.I.T., 1959.

42. Francis, Gordon: Ionization Phenomena in Gases. Academic Press, Inc., 1960.

43. Loeb, Leonard B.: Fundamental Processes of Electrical Discharges in Gases. John Wiley & Sons, Inc., 1939.

44. Kennard, Earle H.: Kinetic Theory of Gases. McGraw-Hill Book Co., Inc., 1938.

45. Gerson, N. C.: A Critical Survey of Ionospheric Temperatures. Rep. on the Prog. in Phys., vol. XXII, The Phys. Soc., 1951, pp. 316-365.

46. Ginsburg, V. L.: On the Absorption of Radio Waves in the Sun's Corona. Astronomical Jour., USSR, vol. 26, no. 2, 1949, pp. 84-96.

47. Nicolet, Marcel: Collision Frequency of Electrons in the Terrestrial Atmosphere. The Phys. of Fluids, vol. 2, no. 2, Mar.-Apr. 1959, pp. 95-99.

48. Smerd, S. F., and Westfold, K. C.: The Characteristics of Radio-Frequency Radiation in an Ionized Gas, with Application to the Transfer of Radiation in the Solar Atmosphere. Phil. Mag., ser. 7, vol. 40, no. 307, Aug. 1949, pp. 831-848.

49. Spitzer, Lyman, Jr.: Physics of Fully Ionized Gases. Interscience Pub., Inc., 1957.

50. Biondi, Manfred, A., and Brown, Sanborn C.: Measurement of Electron-Ion Recombination. Phys. Rev., vol. 76, no. 11, Dec. 1, 1949. pp. 1697-1700.

51. Delcroix, J. L.: Introduction to the Theory of Ionized Gases. Interscience Publishers Inc., 1960.

52. Redfield, A., and Holt, R. B.: Electron Removal in Argon Afterglows. Phys. Rev., vol. 82, no. 6, June 15, 1951, pp. 874-876.

53. Hodgman, Charles D., ed.: Handbook of Chemistry and Physics. Fortieth ed., Chem. Rubber Pub. Co., 1958-1959.

E-1384

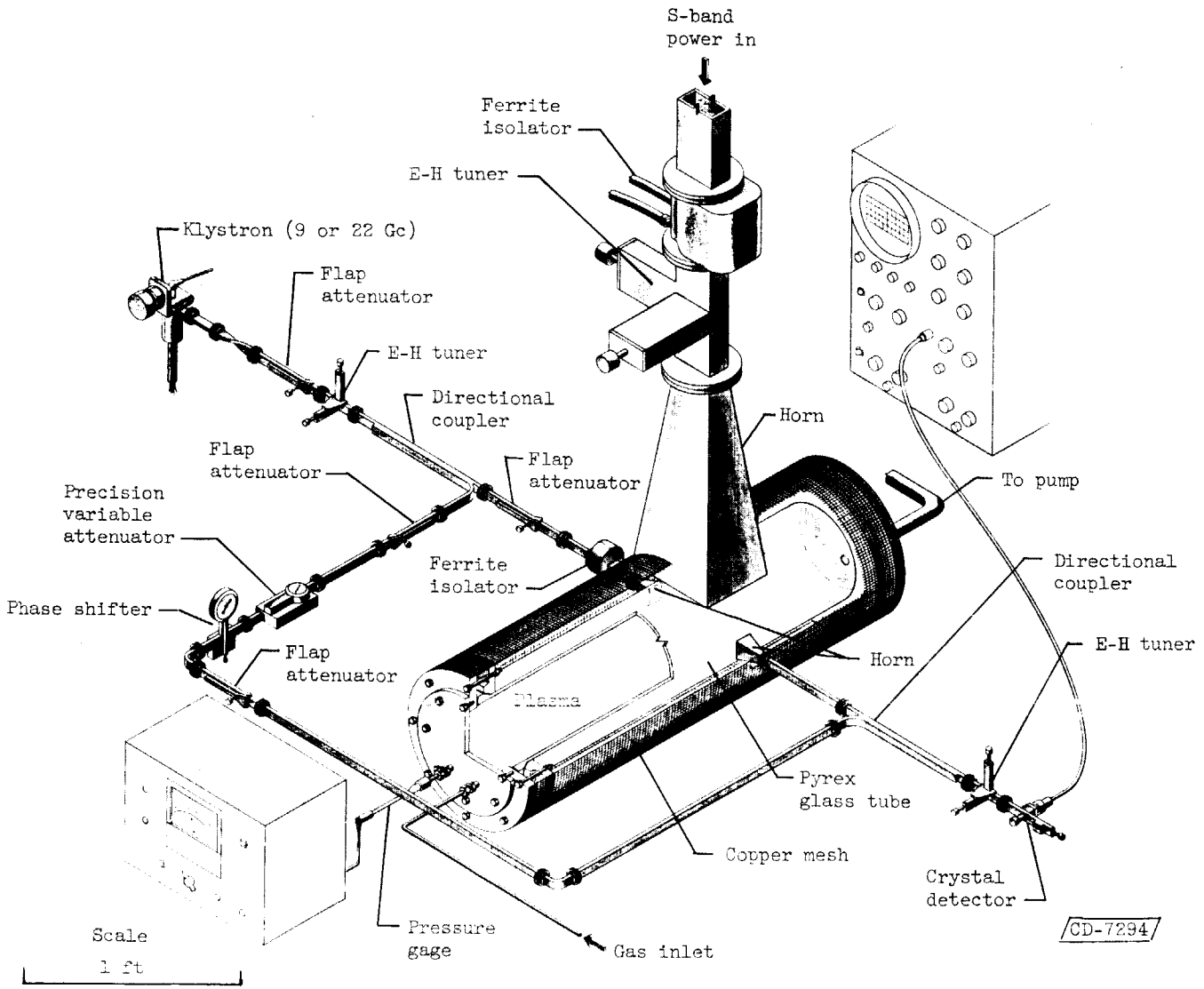

Figure 1. - Diagram of microwave interferometer.

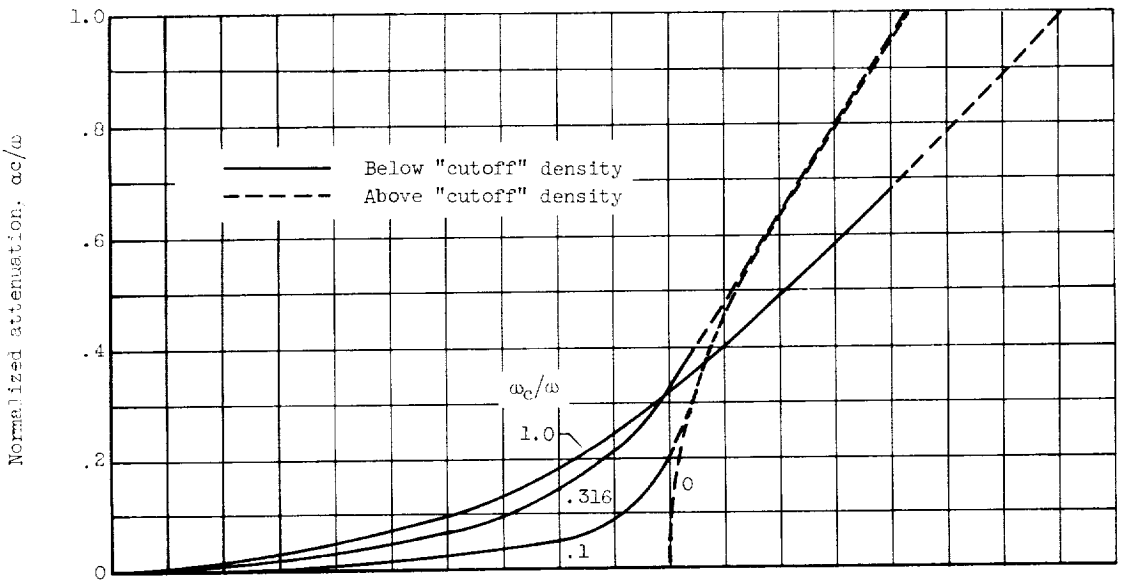

(a) Attenuation.

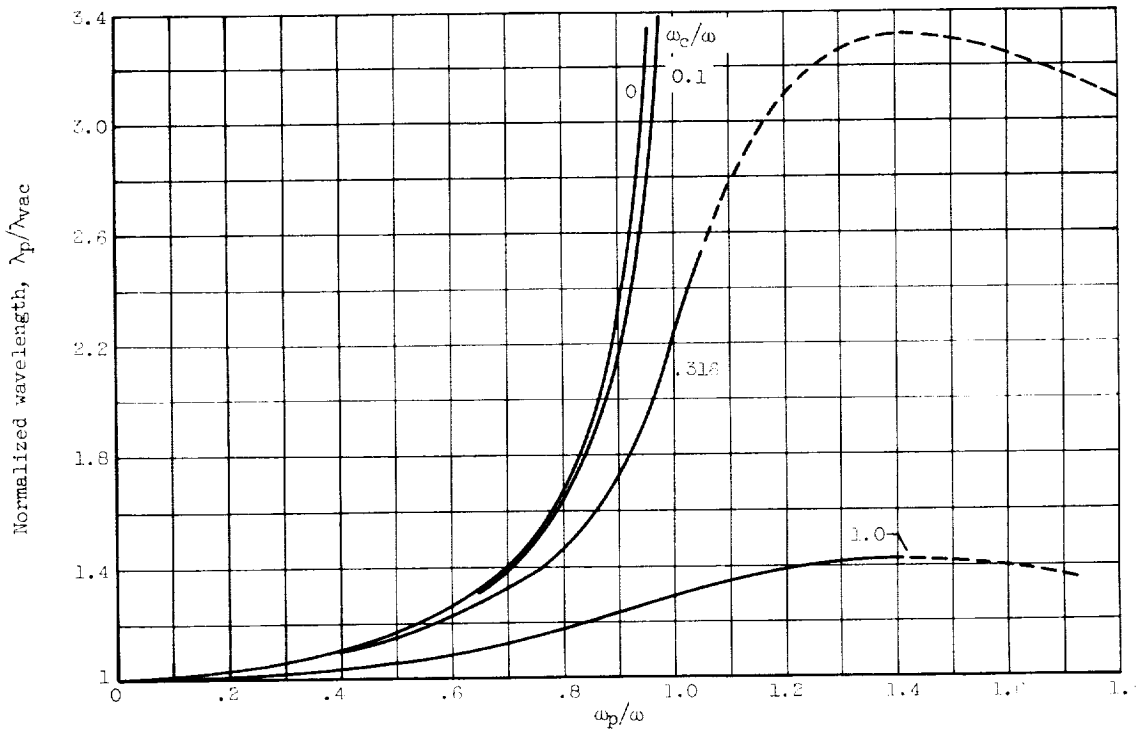

(b) Wavelength.

Figure 2. - Effect of plasma density on attenuation and wavelength. $(\omega_p)^2 = 3.18\times10^{9}\ n_{ee}$.

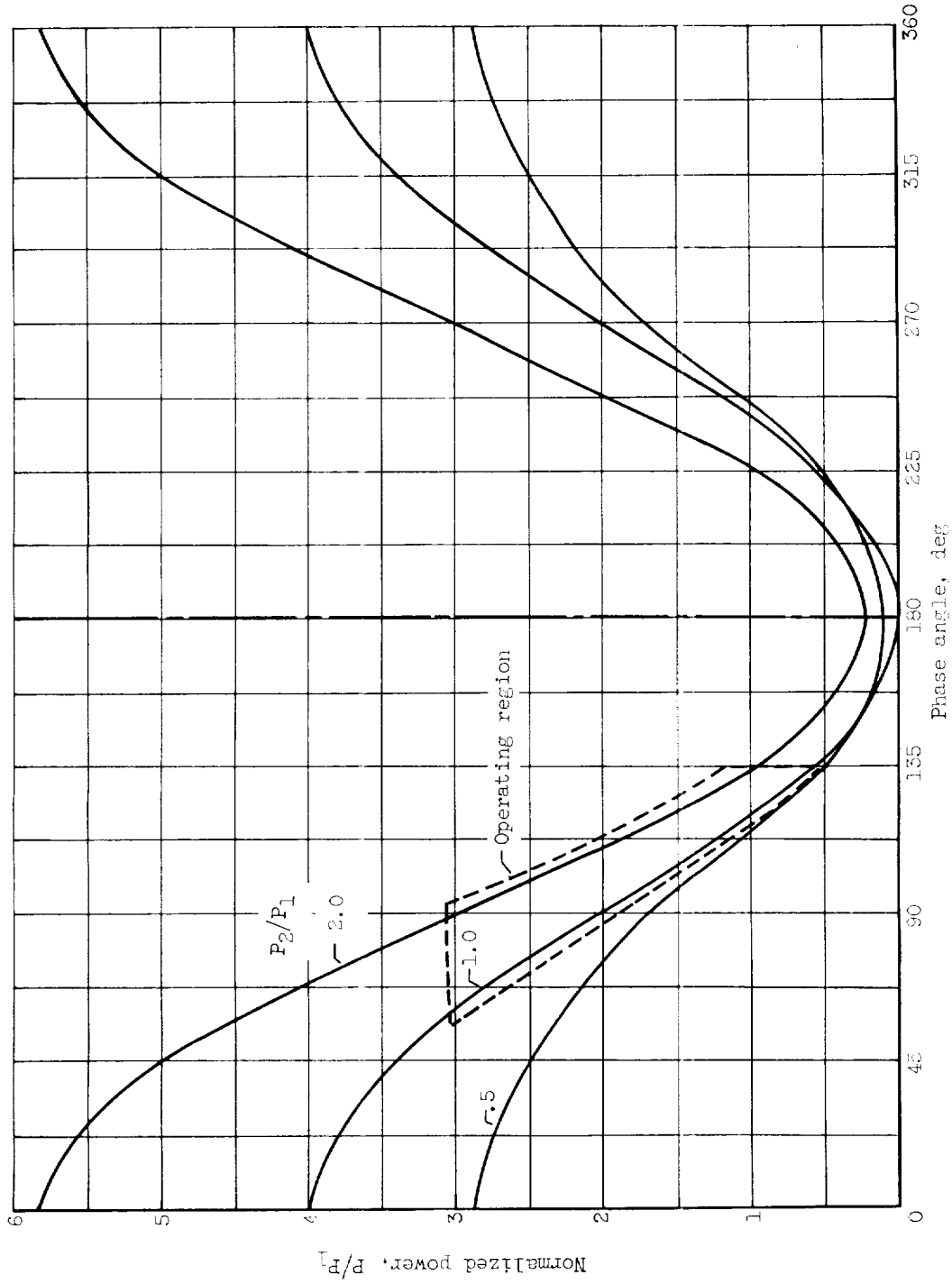

Figure 7. - Normalized total power P/P_1 as a function of phase angle between the two interferometer arms 9.

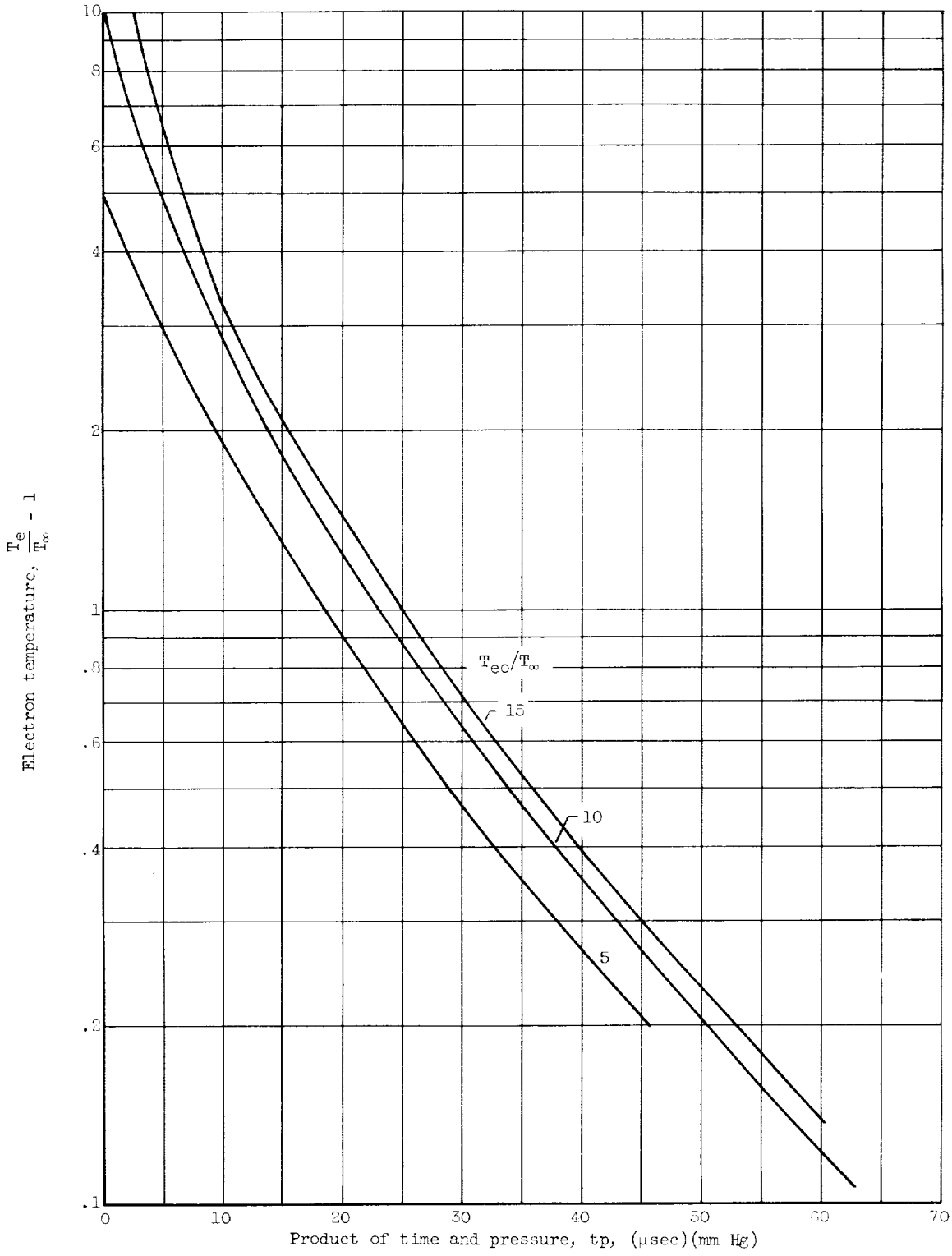

Figure 4. - Decay of electron temperature with time and pressure as a function of electron temperature; nitrogen gas.

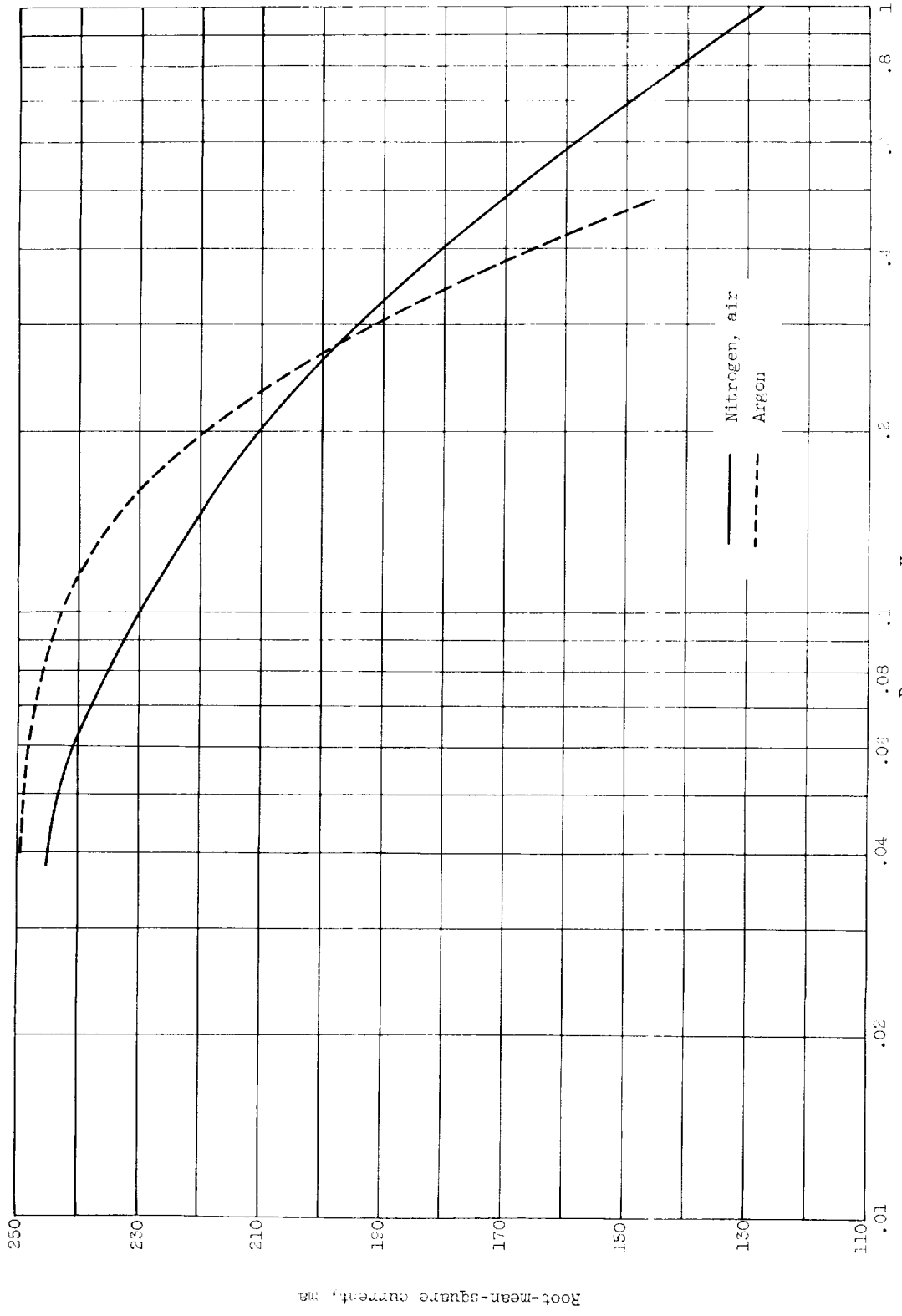

Figure 2. - Current against pressure at 6300 volts. High-voltage abnormal glow discharge.

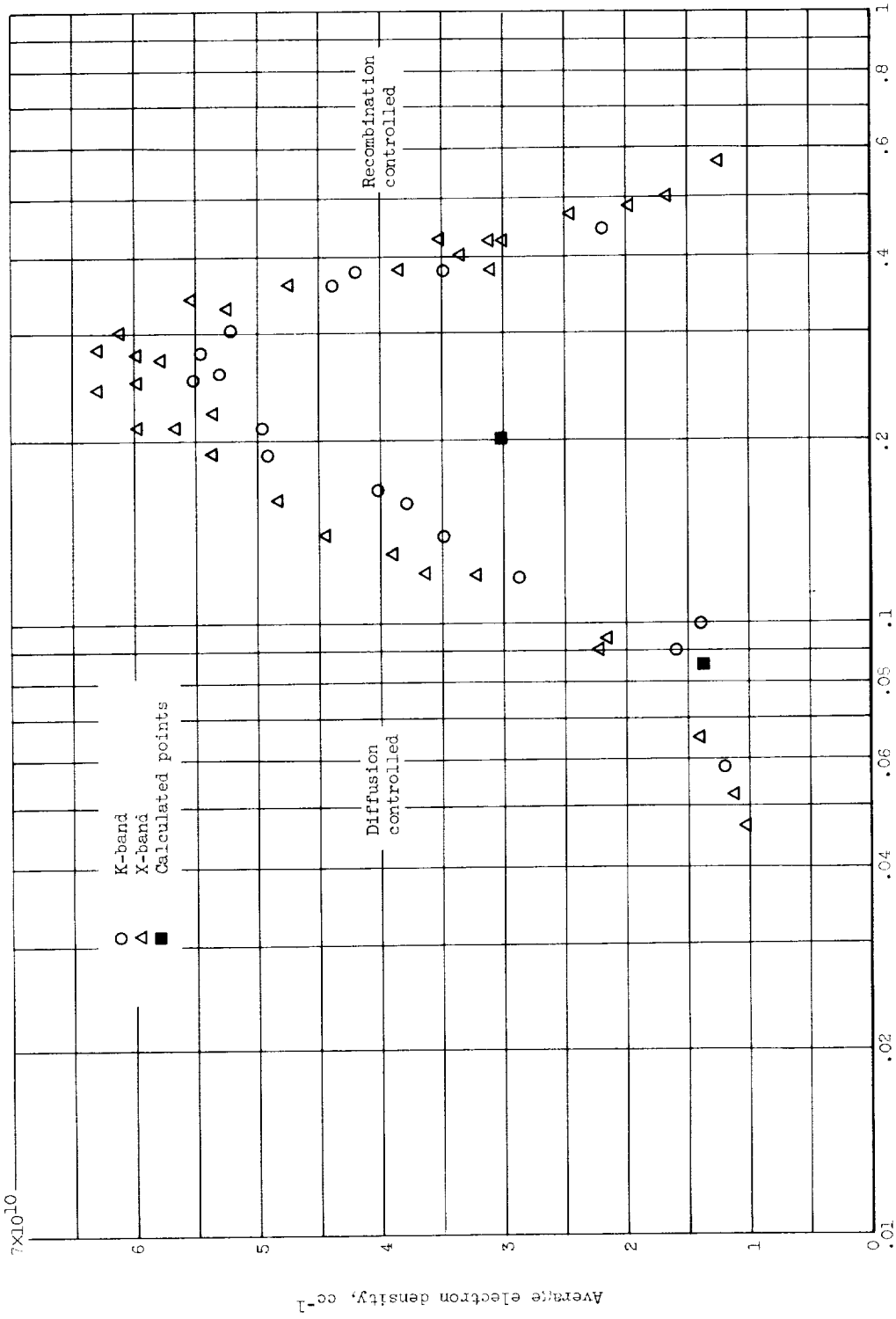

(a) Nitrogen.

Figure 6. - Average electron density of an abnormal glow discharge as a function of pressure.

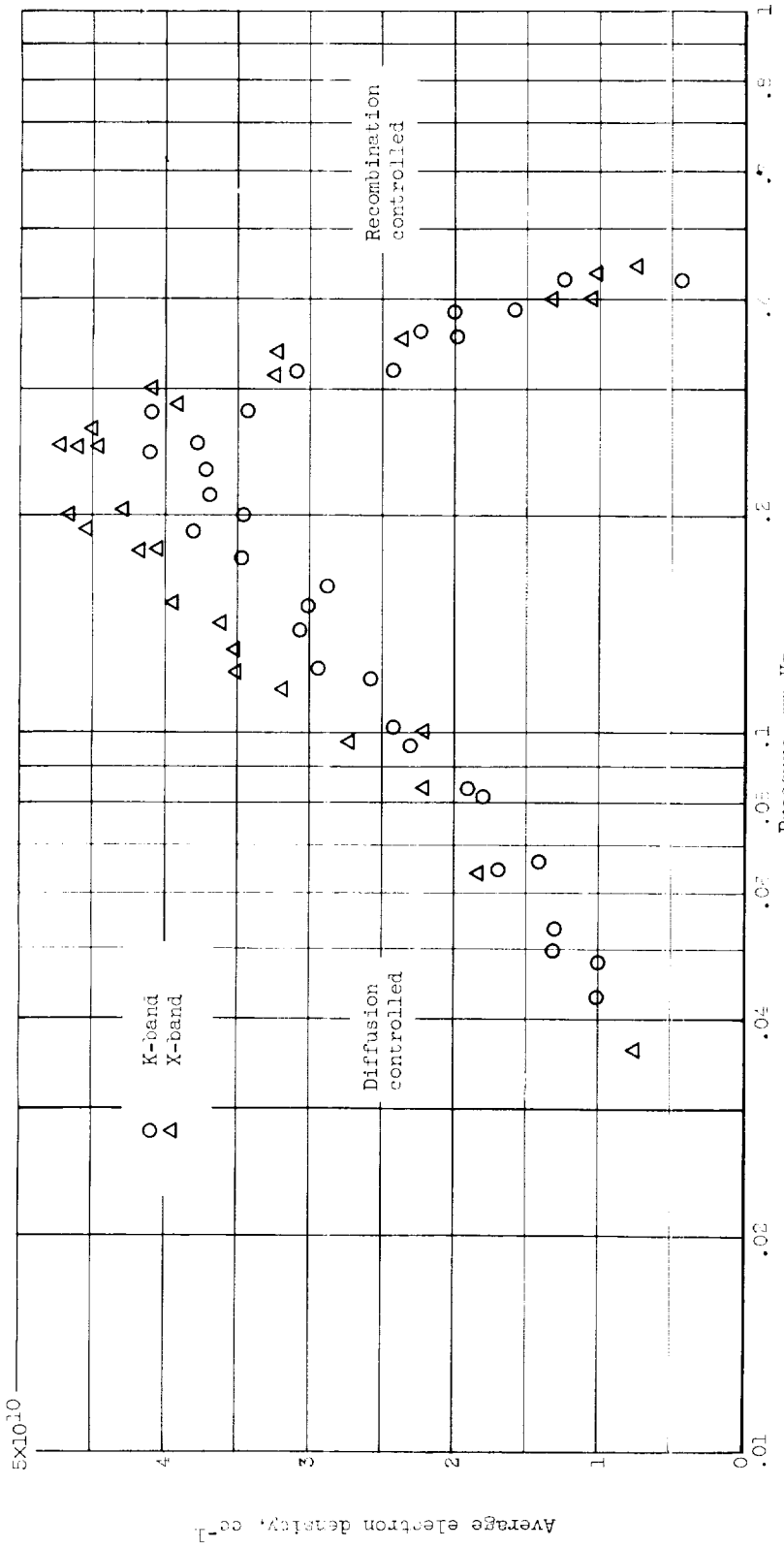

(b) Air.

Figure 6. - Continued. Average electron density of an abnormal glow discharge as a function of pressure.

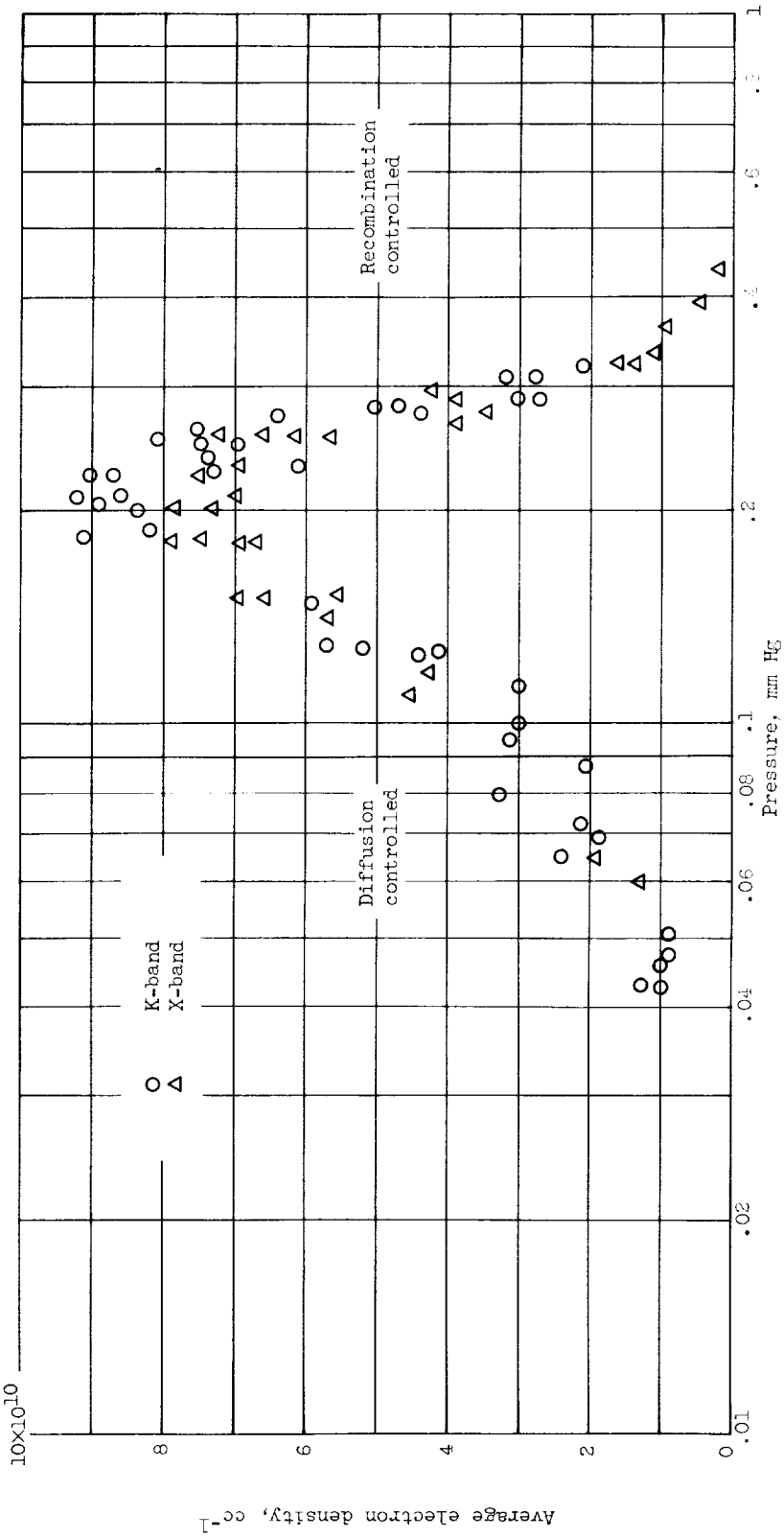

(c) Argon.

Figure 6. - Concluded. Average electron density of an abnormal glow discharge as a function of pressure.

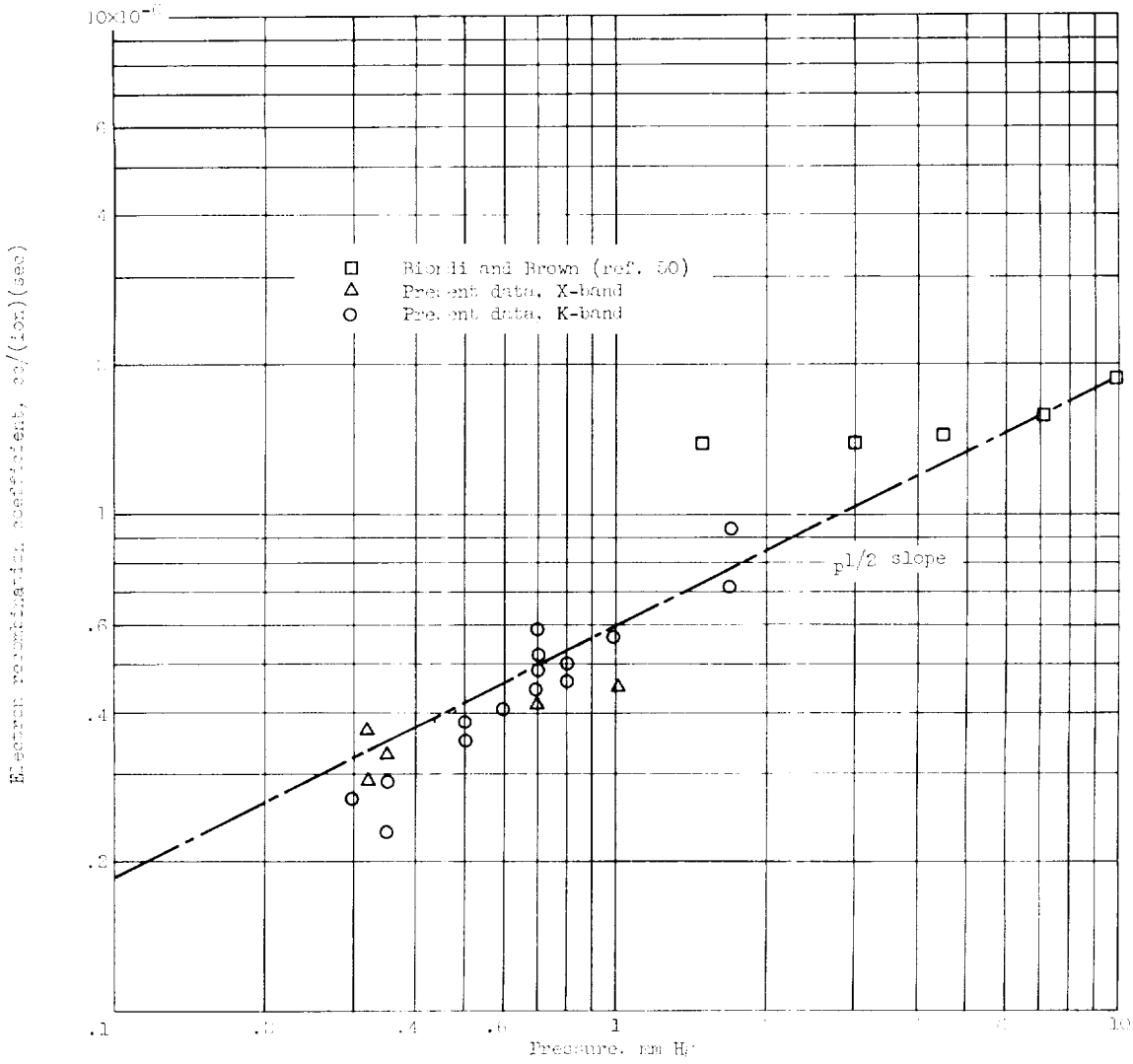

(c) Nitrogen.

Figure 7. - Measured electron-ion recombination coefficient as a function of pressure.

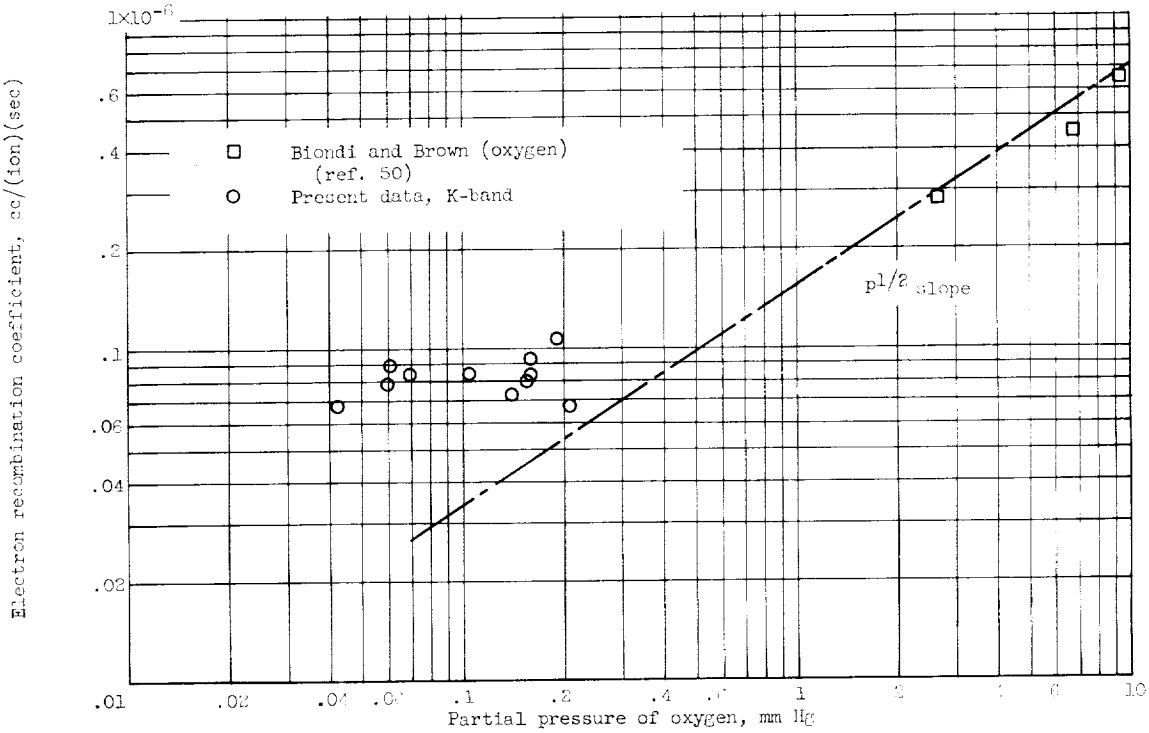

(b) Air.

Figure 7. - Continued. Measured electron-ion recombination coefficient as a function of pressure.

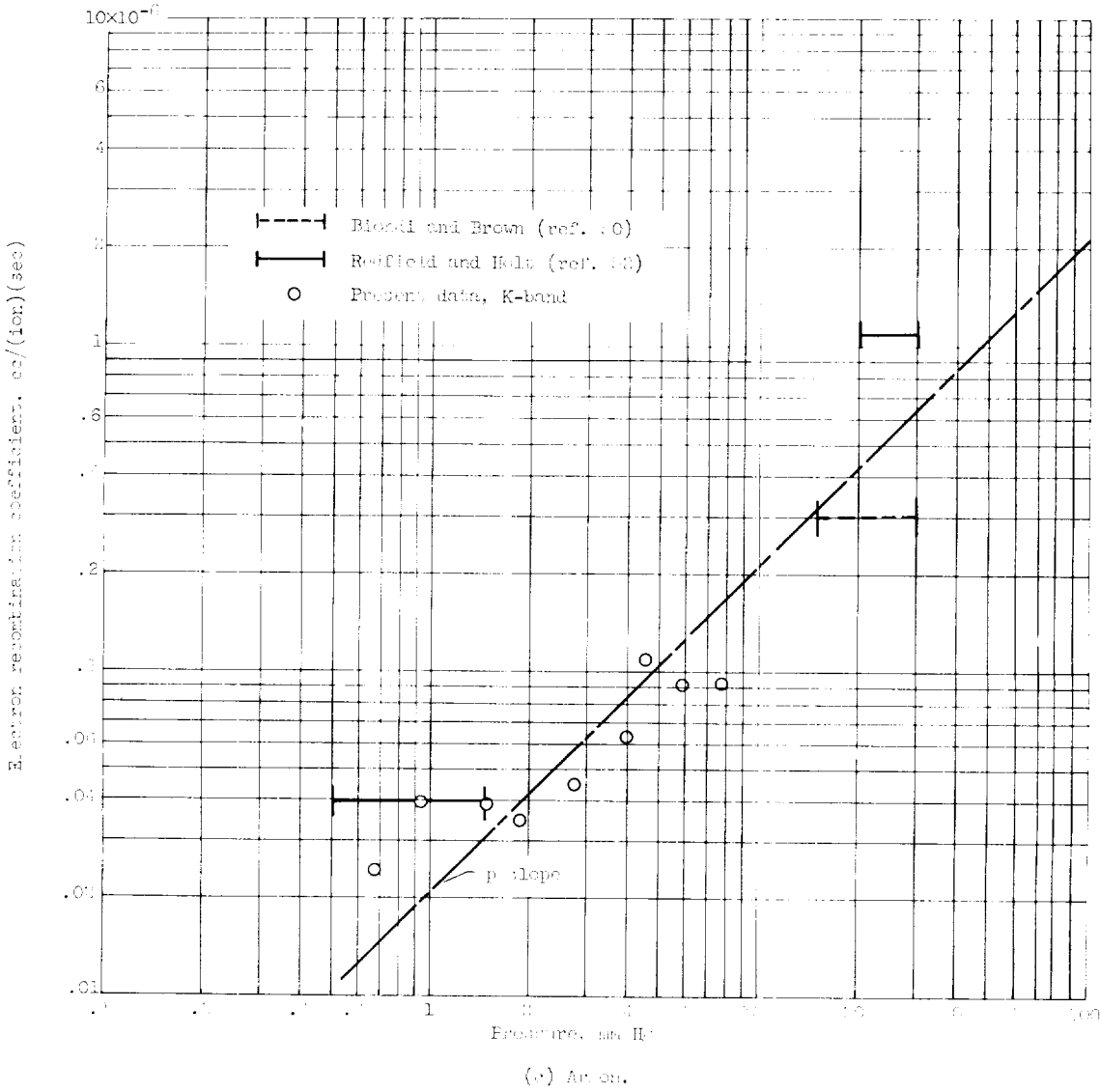

Figure 7. - Concluded. Measured electron-ion recombination coefficient as function of pressure.

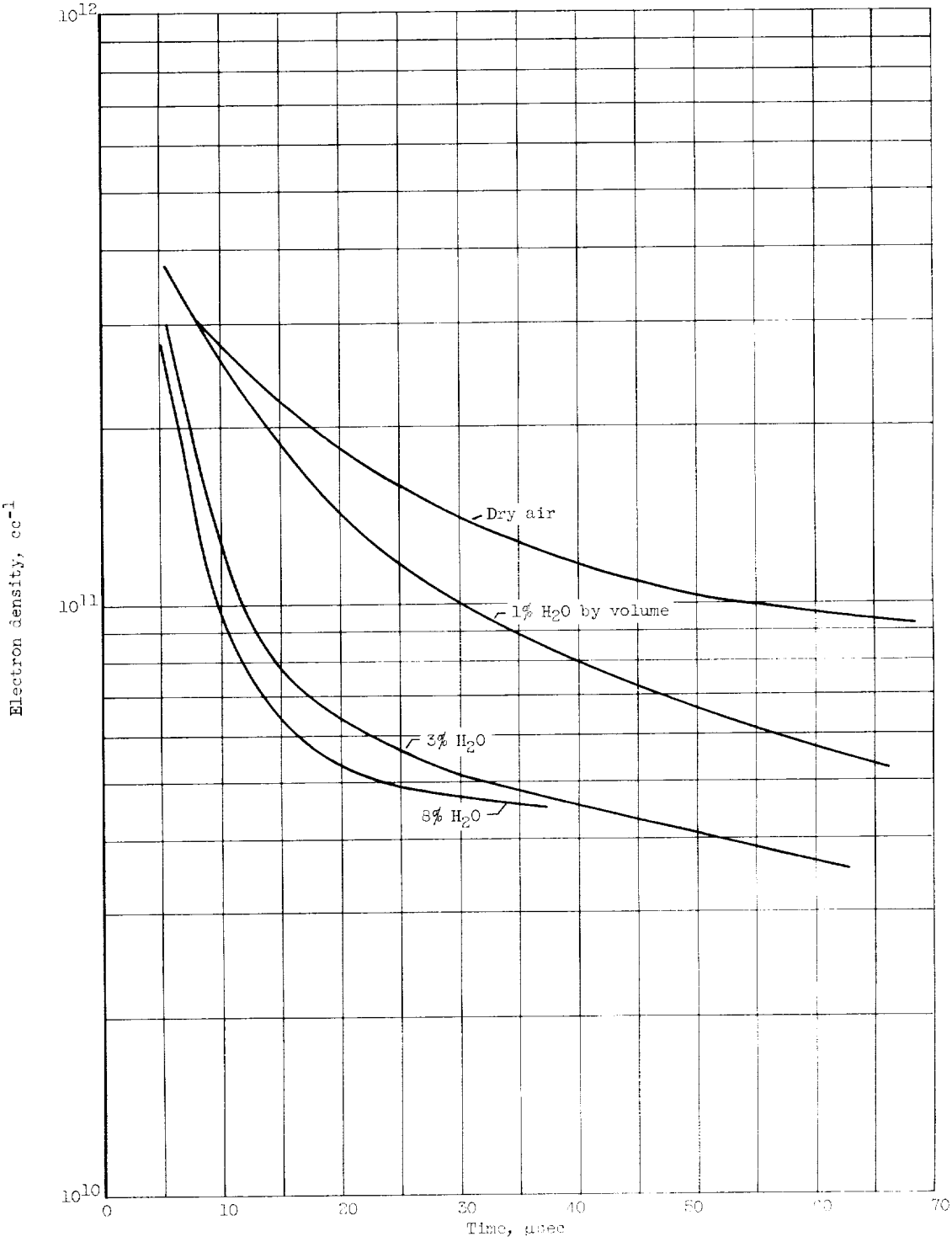

Figure 8. - Typical decay curves after ionizing pulse. Pressure, approximately 0.1 millimeter of mercury.